Canonical ordering for triangulations on the cylinder, with applications to periodic straight-line drawings

Luca Castelli Aleardi, Olivier Devillers, Eric Fusy

▶ To cite this version:

HAL Id: hal-00705181

https://hal.inria.fr/hal-00705181

Canonical ordering for triangulations on the cylinder, with applications to periodic straight-line drawings

Luca Castelli Aleardi*, Olivier Devillers†, Éric Fusy*

Project-Team Geometrica

Abstract: We extend the notion of canonical orderings to cylindric triangulations. This allows us to extend the incremental straight-line drawing algorithm of de Fraysseix et al. to this setting. Our algorithm yields in linear time a crossing-free straight-line drawing of a cylindric triangulation T with n vertices on a regular grid $\mathbb{Z}/w\mathbb{Z} \times [0, h]$, with $w \leq 2n$ and $h \leq n(2d + 1)$, where d is the (graph-) distance between the two boundaries. As a by-product, we can also obtain in linear time a crossing-free straight-line drawing of a toroidal triangulation with n vertices on a periodic regular grid $\mathbb{Z}/w\mathbb{Z} \times \mathbb{Z}/h\mathbb{Z}$, with $w \leq 2n$ and $h \leq 1 + n(2c + 1)$, where c is the length of a shortest non-contractible cycle. Since $c \leq \sqrt{2n}$, the grid area is $O(n^{5/2})$.

Key-words: triangulations, graph drawing, flat torus

* LIX, École Polytechnique, France
† Projet Geometrica, INRIA Sophia-Antipolis, France

Ordre canonique pour des triangulations du cylindre et applications au tracé linéaire de graphes périodiques

Résumé : Nous étendons la notion d'ordre canonique à des triangulations cylindriques. L'algorithme incrémental de tracé de graphe planaire introduit par de Fraysseix et al. peut ainsi être étendu au cas cylindrique. Notre algorithme permet d'obtenir en temps linéaire un tracé linéaire sans croisement d'une triangulation cylindrique T avec n sommets sur la grille régulière $\mathbb{Z}/w\mathbb{Z} \times [0, h]$, où $w \leq 2n$ et $h \leq n(2d+1)$, avec d la distance (en nobre d'arètes de la triangulation) entre les deux bords. On peut en déduire un algorithme en temps linéaire pour un tracé linéaire sans croisement d'une triangulation du tore sur la grille périodique $\mathbb{Z}/w\mathbb{Z} \times \mathbb{Z}/h\mathbb{Z}$, où $w \leq 2n$ et $h \leq 1 + n(2c+1)$, avec c la longueur du plus court cycle non contractible. Comme $c \leq \sqrt{2n}$, l'aire de la grille est en $O(n^{5/2})$.

Mots-clés : triangulations, tracé de graphe, tore plat

1 Introduction

The problem of efficiently computing straight-line drawings of planar graphs has attracted a lot of attention over the last two decades. Two combinatorial concepts for planar triangulations turn out to be the basis of many classical straight-line drawing algorithms: the *canonical ordering* (a special ordering of the vertices obtained by a shelling procedure) and the closely related *Schnyder wood* (a partition of the inner edges of a triangulations into 3 spanning trees with specific incidence conditions). Algorithms based on canonical ordering [7, 10] are typically incremental, adding vertices one by one while keeping the drawing planar. Algorithms based on Schnyder woods [14] are more global, the (barycentric) coordinates of each vertex have a clear combinatorial meaning (typically the number of faces in certain regions associated to the vertex). Algorithms of both types make it possible to draw in linear time a planar triangulation with n vertices on a grid of size $O(n \times n)$. They can also both be extended to obtain (weakly) convex drawings of 3-connected maps on a grid of size $O(n \times n)$. The problem of obtaining planar drawings of higher genus graphs has been addressed less frequently [11, 9, 12, 13, 4, 6, 15], from both the theoretical and algorithmic point of view. Recently some methods for the straight-line planar drawing of genus g graphs with polynomial grid area have been described in [4, 6] (to apply these methods the graph needs to be unfolded planarly along a *cut-graph*). However it does not yield (at least easily) periodic representations: for example, in the case of a torus, the boundary vertices (on the boundary of the rectangular polygon) might not be aligned, so that the drawing does not give rise to a periodic tiling.

Our main contribution is to generalize the notion of canonical ordering and the incremental straight-line drawing algorithm of de Fraysseix et al [7] to triangulations on the cylinder. The obtained straight-line drawing of a cylindric triangulation T with n vertices is x-periodic, on a regular grid of the form $\mathbb{Z}/w\mathbb{Z} \times [0, h]$, with $w \le 2n$ and $h \le n(2d+1)$, where d is the (graph-) distance between the two boundaries. By a reduction to the cylindric case (the reduction is done with the help of a so-called tambourine [2]), we can also obtain a straight-line drawing of a toroidal triangulation T with n vertices on a grid $\mathbb{Z}/w\mathbb{Z} \times \mathbb{Z}/h\mathbb{Z}$, with $w \le 2n$ and $h \le 1+n(2c-1)$, where c is the length of a shortest non-contractible cycle. Since $c \le (2n)^{1/2}$ as shown in [1], we have $h \le (2n)^{3/2}$, so that the grid area is $O(n^{5/2})$.

For the toroidal case we mention that a notion of canonical ordering has been introduced in [5] (this actually works in any genus and yields an efficient encoding procedure) but we do not use it here. We also mention that, independently, an elegant periodic straight-line drawing algorithm for toroidal triangulations has been very recently described in [8], based on so-called *toroidal Schnyder woods* and face-counting operations; in their case the area of the periodic grid is $O(n^4)$.

2 Preliminaries

Graphs embedded on surfaces. A *map* of genus g is a graph (cellularly) embedded on the closed surface of genus g. The map is called *planar* for $g = 0$ (embedding on the sphere) and *toroidal* for $g = 1$ (embedding on the torus). The *dual* of a map G is the map G^* representing the adjacencies of the faces of G, i.e., there is a vertex v_f of G^* in each face f of G, and each edge e of G gives rise to an edge e^* in G^*: if f and f' are the faces on each side of e then e^* connects v_f to $v_{f'}$. A *cylindric map* is a planar map with two marked faces B_1 and B_2 whose boundaries $C(B_1)$ and $C(B_2)$ are simple cycles (possibly $C(B_1)$ and $C(B_2)$ share vertices and edges). The faces B_1 and B_2 are called the *boundary-faces*. Boundary vertices and edges are those belonging to $C(B_1)$ (black circles in Fig. 1) or $C(B_2)$; (red circles in Fig. 1) the other ones are called *inner* vertices (white circles in Fig. 1) and edges.
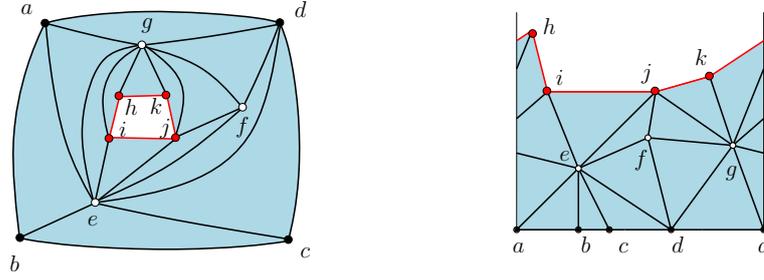
Figure 1: A cylindric triangulation. Left: annular representation. Right: x-periodic representation.

Periodic drawings   Here we consider the problem of drawing a cylindric (resp. toroidal) triangulation on the flat cylinder (resp. flat torus). The flat cylinder is a rectangle with a pair of opposite sides identified; the flat torus is a rectangle with both pairs of opposite sides identified. We classically require coordinates to be integers. So for a cylindric triangulation we aim at a crossing-free straight-line drawing on a regular (x-periodic) grid of the form $\mathbb{Z}/w\mathbb{Z} \times [0, h]$, and for a toroidal triangulation we aim at a crossing-free straight-line drawing on a regular (x-periodic and y-periodic) grid of the form $\mathbb{Z}/w\mathbb{Z} \times \mathbb{Z}/h\mathbb{Z}$.

3   Periodic drawings of cylindric triangulations

We introduce at first a notion of canonical ordering for cylindric triangulations:

Definition 1. *Let G be a cylindric triangulation with boundary-faces B_1 and B_2, and such that the cycle $C(B_1)$ has no chords (i.e., there is no edge that is not on $C(B_1)$ and has both ends on $C(B_1)$). An ordering $\pi = \{v_1, v_2, \ldots, v_n\}$ of the vertices of $G \backslash C(B_1)$ is called a (cylindric) canonical ordering if it satisfies:*

- *For each $k \geq 0$ the map G_k induced by $C(B_1)$ and by the vertices $\{v_1, \ldots, v_k\}$ is a cylindric triangulation. The other boundary-face (the one different from B_1) of G_k, whose contour is denoted C_k, contains B_2 in its interior.*

- *The vertex v_k lies on C_k, and all its neighbors in G_{k-1} appear consecutively on C_{k-1}.*

Shelling procedure. We now describe a shelling procedure to compute a canonical ordering of a cylindric triangulation G with boundary-faces B_1, B_2. At each step the graph formed by the remaining vertices is a cylindric triangulation, one boundary face remains B_1 all the way, while the other boundary-face (initially B_2) has its contour, denoted by C_k, getting closer to $C(B_1)$. A vertex $v \in C_k$ is *free* if v is incident to no chord of C_k and if $v \notin C(B_1)$ (see Fig. 2 top left). The shelling procedure goes as follows (n is the number of vertices in $G \backslash C(B_1)$): for k from n to 1, choose a free vertex v on C_k, assign $v_k \leftarrow v$, and then delete v together with all its incident edges. The existence of a free vertex at each step follows from the same argument as in the planar case [3]. Indeed, if there is no chord incident to C_k, then any vertex $v \in C_k$ is free, while if there is a chord e for C_k, then the set of chords incident to C_k forms a system of archs (relative to C_k). If we look at a chord $e = \{u, v\}$ that is "innermost" (i.e., no other chord is nested inside e), then the path between u and v on C_k contains at least one vertex, which has to be free (see Fig. 2 top right).
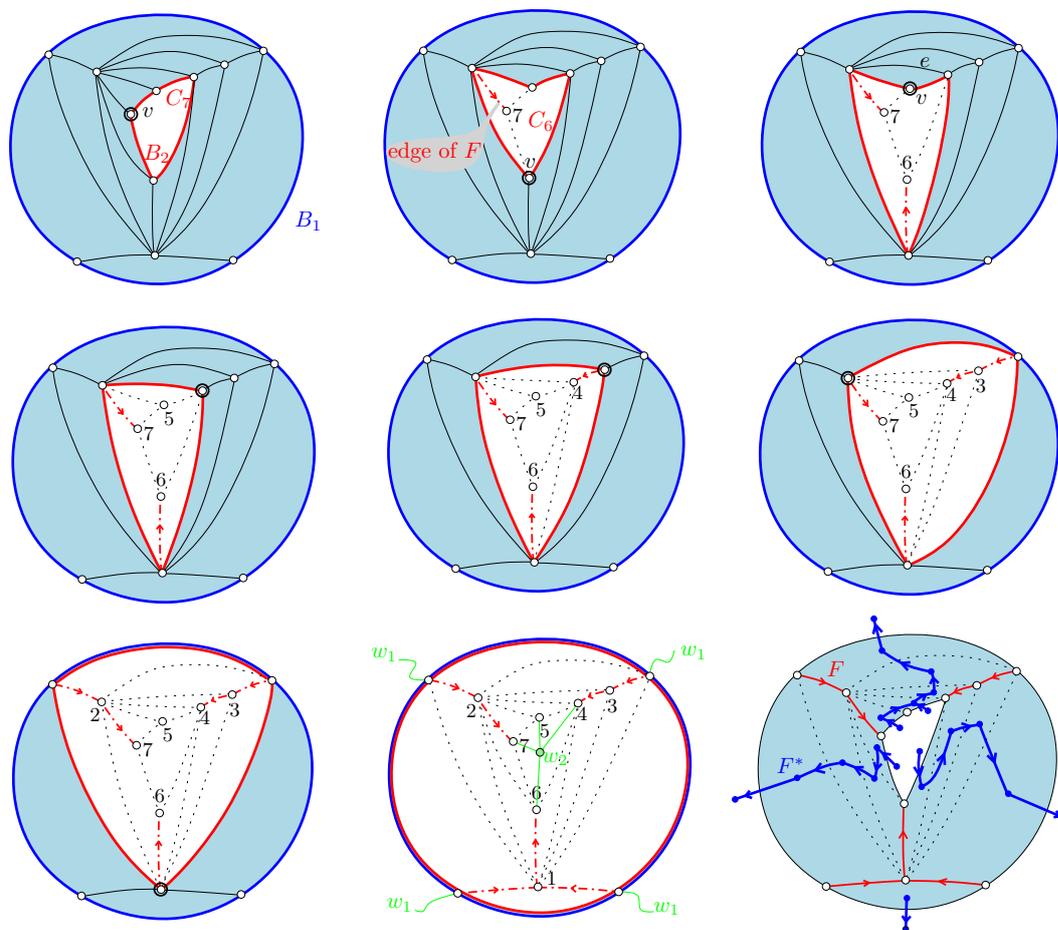
Figure 2: Shelling procedure to compute a canonical ordering of a given cylindric triangulation. The underlying forest is computed on the fly; the last drawing shows the underlying forest superimposed with the dual forest. The graph is the one of Fig. 1.

Underlying forest and dual forest. Given a cylindric triangulation G (with boundary faces B_1 and B_2) endowed with a canonical ordering π, define the *underlying forest* F for π as the oriented subgraph of G where each vertex $v \in C(B_2)$ has outdegree 0, and where each $v \notin C(B_2)$ has exactly one outgoing edge, which is connected to the adjacent vertex of v of largest label in π. (The forest F can be computed on the fly during the shelling procedure: when treating a free vertex v with neighbours $c_p, \ldots, c_q$ from left to right, add the edges $\{c_i, v\}$ to F, these edges being oriented toward v.) Since the edges are oriented in increasing labels, F is an oriented forest; it spans all vertices of $G \backslash C(B_2)$ and has its sinks on $C(B_2)$. The *augmented map* $\widehat{G}$ is obtained from G by adding a vertex w_1 inside B_1, a vertex w_2 inside B_2, and connecting all vertices around B_1 to w_1 and all vertices around B_2 to w_2 (thus triangulating the interiors of B_1 and B_2, see Fig. 2 bottom middle). Define $\widehat{F}$ as F plus all edges incident to w_1 and all edges incident to w_2. Define the *dual forest* F^* for π as the graph formed by the vertices of $\widehat{G}^*$ (the dual of $\widehat{G}$) and by the edges of $\widetilde{G}^*$ that are dual to edges not in $\widehat{F}$. Since $\widehat{F}$ is a spanning
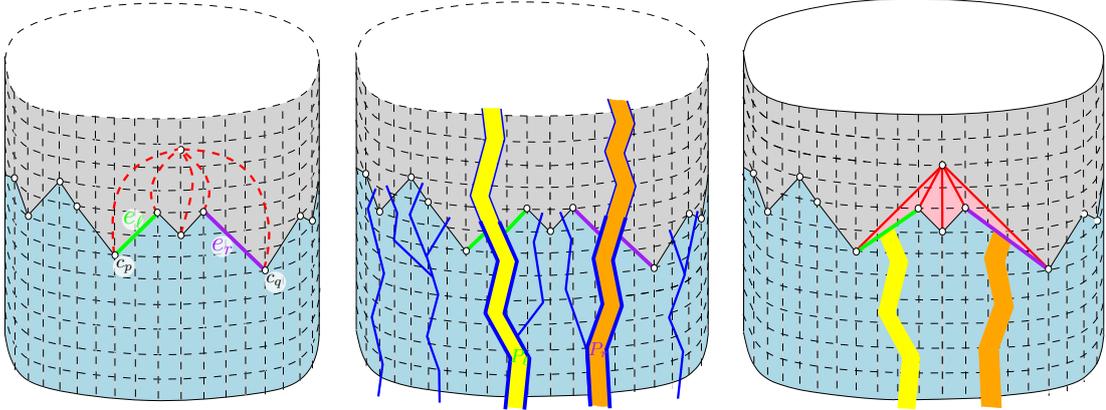
Figure 3: One step of the incremental drawing algorithm. Two vertical strips of width 1 (each one along a path in the dual forest) are inserted in order to make the slopes of e_ℓ and e_r smaller than 1 in absolute value. Then the new vertex and its edges connected to the upper boundary can be drawn in a planar way.

connected subgraph of $\widehat{G}$, F^* is a spanning tree of $\widetilde{G}^*$. Precisely each of the trees (connected components) of F^* is naturally rooted at a vertex "in front of" each edge of B_1, and the edges of the tree can naturally be oriented toward this root-vertex (see Fig. 2 bottom right).

Drawing algorithm. Given a cylindric triangulation G with no chordal edge incident to B_1, we first compute a canonical ordering of G, and then draw G in an incremental way. We start with a cylinder of width $2|C(B_1)|$ and height 0 (i.e., a circle of length $2|C(B_1)|$) and draw the vertices of $C(B_1)$ equally spaced on the circle (space 2 between two consecutive vertices). Then the strategy is —for each $k \geq 1$— to compute the drawing of G_k out of the drawing of G_{k-1} by first stretching the cylinder (increasing the width by 2) and then placing the vertex v_k and its incident edges (in G_k) in a planar way. Define the *x-span* of an edge e in the cylindric drawing as the number of columns $[i, i+1] \times [0, +\infty]$ that meet the interior of e (we have no need for a more complicated definition since, in our drawings, a column will never meet an edge more than once).

Consider the dual forest F^* for the canonical ordering restricted to G_{k-1}. Let $c_p, c_{p+1}, \ldots, c_q$ be the path of C_{k-1} such that C_{k-1} is on the left of the path taking from c_p to c_q. Let e_ℓ be the edge $\{c_p, c_{p+1}\}$ and e_r be the edge $\{c_{q-1}, c_q\}$ (note that $e_\ell = e_r$ if $q - p = 1$). Let P_ℓ (resp. P_r) be the path in F^* from e_ℓ^* (resp. e_r^*) to the root in its connected component (which is a vertex "in front of" an edge of B_1). We stretch the cylinder by inserting a vertical strip of length 1 along P_ℓ and another along P_r (see Fig. 3). The effect is exactly to increase by 1 the x-span of each edge dual to an edge in P_ℓ, and then to increase by 1 the x-span of each edge dual to an edge in P_r (note that P_ℓ and P_r are not necessarily disjoint, in which case the x-span of an edge dual to an edge in $P_\ell \cap P_r$ is increased by 2, see Fig. 7 second on line3). After these stretching operations, whose effect is to make the slopes of e_ℓ and e_r strictly smaller than 1 in absolute value, we insert (as in the planar case) the vertex v_k at the intersection of the ray of slope 1 starting from c_p and the ray of slope -1 starting from c_q, and we connect v_k to $c_p, \ldots, c_q$ by segments [1]. These two

---

[1]In the de Fraysseix et al algorithm for planar triangulations, the step to make the (absolute value of) slopes of e_ℓ and e_r smaller than 1 is formulated as a shift of certain subgraphs described in terms of the underlying forest F. The extension of this formulation to the cylinder would be quite cumbersome. We find the alternative formulation as strip insertions more convenient for the cylinder (it also gives rise to a very easy linear implementation).
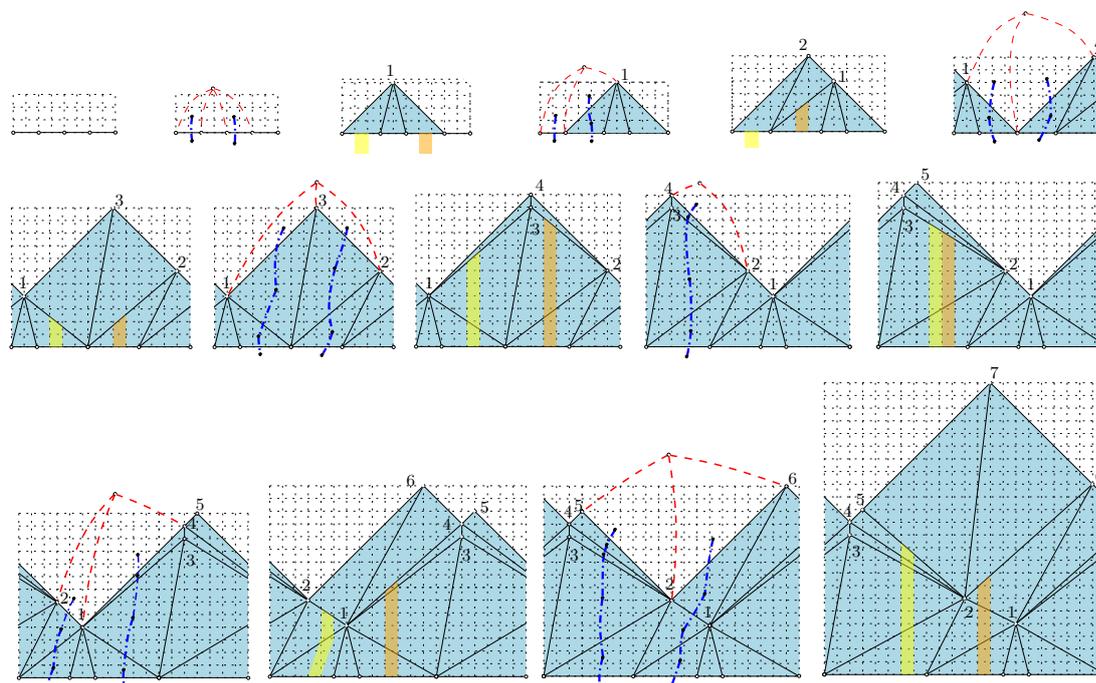
Figure 4: Algorithm (Prop. 2) to compute an x-periodic drawing of a cylindric triangulation (no chordal edges incident to C_0). The vertices are treated in increasing label (the canonical ordering is the one computed in Fig. 2).

rays actually intersects at a grid point since the Manhattan distance between any two vertices on C_{k-1} is even.Fig. 7 shows the execution of the algorithm on the example of Fig. 1.

Proposition 2. *For each cylindric triangulation G with no chordal edges incident to $C(B_1)$, one can compute in linear time a crossing-free straight-line drawing of G on an x-periodic regular grid $\mathbb{Z}/w\mathbb{Z} \times [0, h]$ where —with n the number of vertices of G and d the (graph-)distance between the two boundaries— $w = 2n$ and $h \leq n(2d + 1)$, such that: every $v \in C(B_1)$ has $y(v) = 0$ (so every edge in $C(B_1)$ has slope 0), and every edge belonging to $C(B_2) \backslash C(B_1)$ has slope ± 1.*

Proof. The fact that the drawing remains crossing-free relies on the slope-property for the upper boundary and on the following inductive property that is easily shown to be maintained at each step k from 1 to n:

> **Pl**: for each edge e on C_k (the upper boundary of G_k), let P_e be the path in F^* from e^* to the root, let E_e be the set of edges dual to edges in P_e, and let δ_e be any positive integer. Then the drawing remains planar when successively increasing by δ_e the x-span of all edges of E_e, for all $e \in C_k \backslash \{a, b\}$.

We now prove the bounds on the grid-size. If $|C(B_1)| = t$ then the initial cylinder is $2t \times 0$; and at each vertex insertion, the grid-width grows by 2. Hence $w = 2n$. In addition, due to the slope conditions (slopes of boundary-edges are at most 1 in absolute value), the y-span (vertical span) of every edge e is not larger than the current width at the time when e is inserted in the drawing. Hence, if we denote by v the vertex of $C(B_2)$ that is closest (at distance d) to $C(B_1)$,
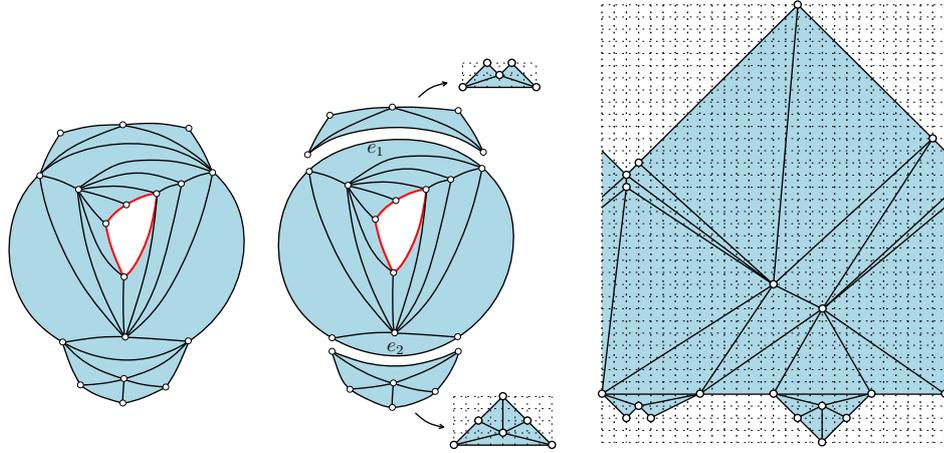
Figure 5: Drawing a cylindric triangulation with chords at B_1. To make enough space to place the component under e_2, one takes 8 (instead of 2) as the initial x-span of e_2.

then the ordinate of v is at most $d \cdot (2n)$. And due to the slope conditions, the vertical span of $C(B_2)$ is at most $w/2 \leq n$. Hence the grid-height is at most $n(2d+1)$. The linear-time complexity is shown next.   □

Linear-time implementation. An important remark is that, instead of computing the x-coordinates and y-coordinates of vertices in the drawing, one can compute the y-coordinates of vertices and the x-span of edges (as well as the knowledge of which extremity is the left-end vertex and which extremity is the right-end vertex). In a first pass (for k from 1 to n) one computes the y-coordinate of vertices and the x-span r_e of each edge $e \in G$ at the time $t = k$ when it appears on G_k (as well one gets to know which extremity of e is the left-end vertex). Afterward, and if $e \notin F$, the x-span of e might further increase due to insertion of new vertices. Precisely let v_j be a vertex inserted afterwards (i.e., $j > t$), let $c_p, \ldots, c_q$ be its neighbours in G_{j-1} from left to right, let $e_\ell = \{c_p, c_{p+1}\}$, $e_r = \{c_{q-1}, c_q\}$, and let $e'_\ell = \{v_j, c_p\}$ and $e'_r = \{v_j, c_q\}$. Note that e is stretched due to the insertion of the strip along P_ℓ iff either $e = e_\ell$ or e_ℓ is in the subtree of F^* formed by the edges descending from e^*. This happens iff e'_ℓ is in the subtree T_e of F^* formed by the edges descending from e^*. Similarly e is stretched due to the insertion of the strip along P_r iff e'_r is in T_e. To state it more clearly, each edge in T_e is responsible for an increase (by 1) of the x-span of e. Hence the total x-span of each edge $e \in G$ is given by $r_e + s_e$, where $s_e = 0$ if $e \in F$, and, if $e \notin F$, s_e is the number of edges in T_e. Since all quantities s_e can easily be computed in linear time, this gives a linear implementation.

Allowing for chordal edges at B_1. We finally explain how to draw a cylindric triangulation when allowing for chordal edges incident to $C_0 = C(B_1)$; it is good to view B_2 as the top boundary-face and B_1 as the bottom-boundary face (and imagine a standing cylinder). For each chordal edge e of C_0, the *component under* e is the face-connected part of G that lies below e; such a component is a quasi-triangulation (polygonal outer face, triangular inner faces) rooted at the edge e. A chordal edge e of C_0 is *maximal* if the component Q_e under e is not strictly included in the component under another chordal edge. The *size* of such an edge e is defined as $|e| = |V(Q_e)| - 2$. (the size $|e|$ is actually the width of the drawing of Q_e using the de Fraysseix et al algorithm [7]). If we delete the component under each maximal chordal edge (i.e., delete

everything from the component except for the chordal edge itself) we get a new bottom cycle C_0' that is chordless, so we can draw the reduced cylindric triangulation G' using the algorithm of Proposition 2. As we have seen in Section 3 (linear implementation paragraph), for each edge e of C_0', the initial x-stretch is $r_e = 2$ and then the further increase s_e of the x-stretch equals the number of edges descending from e^* in the dual forest F^*. Note that we have actually some freedom to choose the initial x-stretch r_e of each edge on $e \in C_0'$ (just it has to be a positive even number, since at each step of the incremental algorithm the vertices of the current upper boundary have to be at even Manhattan distance). If $e \in C_0$ (i.e., e was not chordal in G) we take $r_e = 2$. If $e \notin C_0$ (i.e., e was a maximal chordal edge in G), we take for r_e the minimal even positive number such that $r_e + s_e \geq |e|$, i.e., $r_e = 2 \cdot \max(1, \lceil(|e| - s_e)/2\rceil)$. Hence, at the end of the execution of the drawing of G', the length $\ell_e = r_e + s_e$ of each maximal chord e satisfies $\ell_e \geq |e|$. Then for each maximal chord e of C_0, we draw the component Q_e under e using the planar algorithm by de Fraysseix et al [7]. this drawing has width $|e|$, with e as horizontal bottom edge of length $|e|$ and with the other outer edges of slopes ± 1. We shift the left-extremity of e so that the drawing of Q_e gets width $\ell(e)$, then we rotate the drawing of Q_e by 180 degrees and plug it into the drawing of G' (see Fig. 5). The overall drawing of G thus obtained is clearly planar. We obtain:

Theorem 3. *For each cylindric triangulation G, one can compute in linear time a crossing-free straight-line drawing of G on an x-periodic regular grid $\mathbb{Z}/w\mathbb{Z} \times [0, h]$, where —with n the number of vertices and d the (graph-) distance between the two boundaries— $w \leq 2n$ and $h \leq n(2d + 1)$. The drawing is vertically convex (the intersection with each vertical line is a segment) and the slopes of boundary-edges are at most 1 in absolute value.*

4   Periodic drawings of toroidal triangulations

For a toroidal triangulation G, a *tambourine* is a pair of parallel (i.e., homotopically equivalent) non-contractible oriented cycles Γ_1 and Γ_2 such that the edges arriving to Γ_1 from the right depart at Γ_2 and the edges arriving to Γ_2 from the left depart at Γ_1 It can be shown (see [2] and the next paragraph) that for each non-contractible cycle Γ of G, there exists a tambourine whose two cycles are parallel to Γ. Deleting the edges that are strictly inside the tambourine, one obtains a cylindric triangulation G' with Γ_1 and Γ_2 as the contours of the boundary-faces. Note also that the distance d between Γ_1 and Γ_2 is smaller than the length of a shortest non-contractible cycle not parallel to Γ. We now apply the algorithm of Theorem 3 to G'. If augment the height h of the drawing to $h' = h + w + 1$, and then wrap the x-periodic grid $\mathbb{Z}/w\mathbb{Z} \times [0, h]$ into a periodic grid $\mathbb{Z}/w\mathbb{Z} \times \mathbb{Z}/h'\mathbb{Z}$, and finally insert the edges inside the tambourine as segments [2], then the slope properties (edges on Γ_1 and Γ_2 have slope at most 1 in absolute value while edges inside the tambourine have slope greater than 1 in absolute value) ensure that the resulting drawing is crossing-free (see Fig. 6).

An important remark is that we can choose Γ so that the graph-distance between the two boundaries Γ_1 and Γ_2 (in G') is smaller that the length γ of a shortest non-contractible cycle in G; and this choice for Γ can be done without computing a shortest non-contractible cycle. Let $\{\Gamma_a, \Gamma_b\}$ be a basis of non-contractible cycles (which can be found in linear time by computing for instance a cut-graph). Denoting by Γ_{min} a shortest non-contractible cycle of G, for sure at least one of Γ_a or Γ_b is not parallel to Γ_{min}. Hence, for Γ_a or for Γ_b, the distance between the boundary-cycles (after deleting edges of the parallel tambourine) is smaller than $|\Gamma_{min}|$. In other

---

[2]We insert the edges in the tambourine T in the unique way such that, looking from bottom to top, at least one edge in T goes strictly to the right, and all edges going strictly to the right have x-span at most w; in this way it is easy to check that the x-span of all edges in T is at most w.
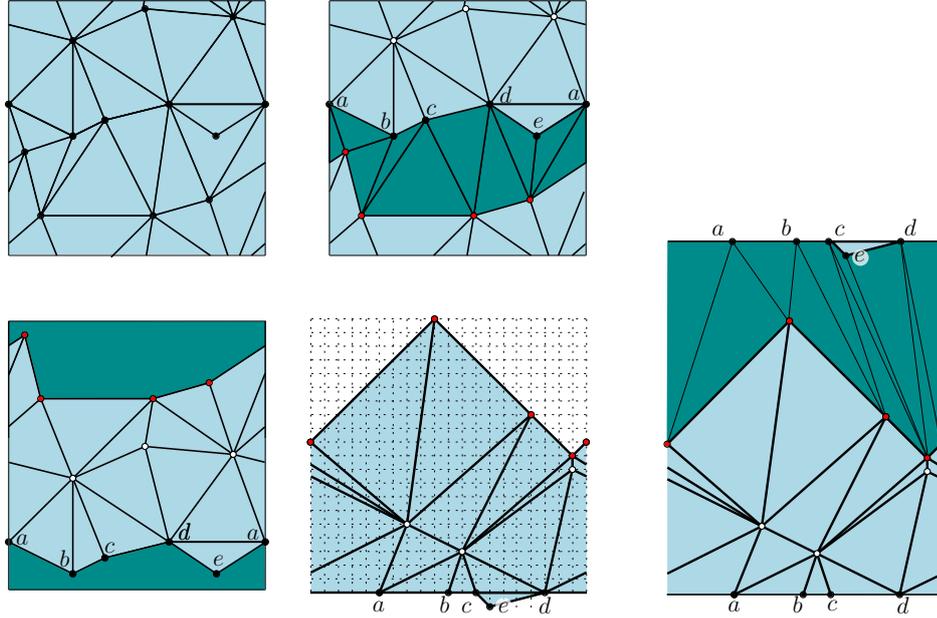
Figure 6: The main steps for drawing of a toroidal triangulation : 1) remove the edges inside a tambourine, (2) draw the obtained cylindric triangulation, 3) insert the edges of the tambourine back into the drawing.

words if we choose the one cycle (among $\{\Gamma_a, \Gamma_b\}$) that yields the smaller distance between the two boundaries of G', then this distance will be smaller than γ. We obtain:

Theorem 4. *For each toroidal triangulation G, one can compute in linear time a crossing-free straight-line drawing of G on a periodic regular grid $\mathbb{Z}/w\mathbb{Z} \times \mathbb{Z}/h\mathbb{Z}$, where —with n the number of vertices and γ the length of a shortest non-contractible cycle— $w \le 2n$ and $h \le 1 + n(2\gamma + 1)$. Since $\gamma \le \sqrt{2n}$ (as shown in [1]), the grid area is $O(n^{5/2})$.*

Existence of a tambourine. For the sake of completeness we include a proof of existence of a tambourine, which slightly extends the proof given in the master's thesis of Arnaud Labourel. A toroidal map is called *weakly 3-connected* if its periodic representation in the plane is 3-connected. Let G be such a map and let Γ be a non-contractible cycle of G. We are going to show that G has a tambourine parallel to Γ. Let G' be the cylindric map obtained after cutting G along Γ; we take the annular representation of G', calling Γ_1 (resp. Γ_2) the copy of Γ that is the outer (resp. inner) boundary. Let Γ' be the smallest (in terms of the enclosed area) cycle that strictly encloses Γ_2 (i.e., encloses Γ_2 and is vertex-disjoint from Γ_2). Let Γ'' be the largest (in terms of the enclosed area) cycle that is strictly enclosed in Γ' (i.e., is enclosed by Γ' and is vertex-disjoint from Γ'). Note that by minimality Γ' has no chord inside, and by maximality Γ'' has no chord outside. Hence if we can show that there is no vertex in the area A (strictly) between Γ' and Γ'' then we can conclude that, in G, Γ' and Γ'' form a tambourine parallel to Γ. Assume there is a vertex v in A. Call *vertex of attachment* for Γ' a vertex w such that there is a path from v to w visiting only vertices of A before reaching w. Again by minimality of Γ' it is easy to see that there is a unique vertex of attachment v' for Γ'. Similarly (by maximality of Γ'') there is a unique vertex of attachment v'' for Γ''. Let Γ_v be the connected component of $G'\backslash\{v', v''\}$ that
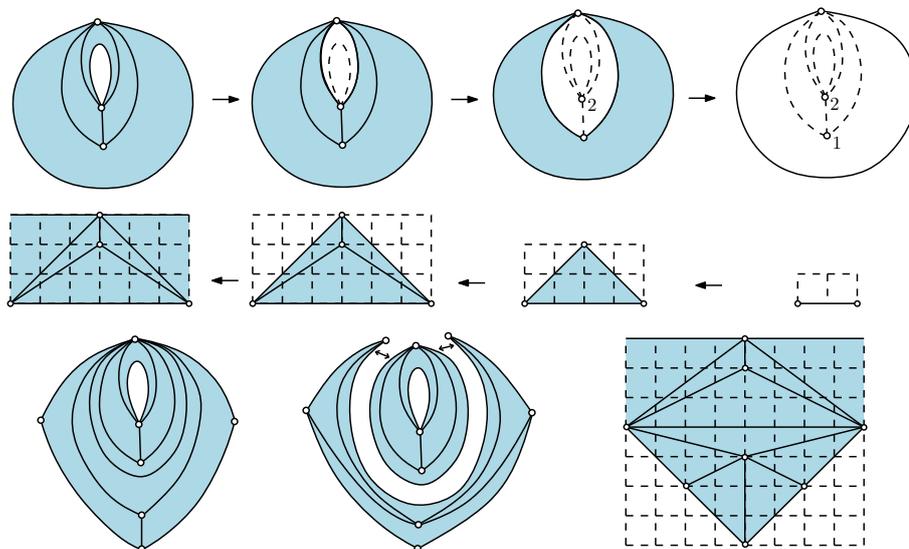
Figure 7: Top line: canonical ordering of a cylindric triangulation with non-contractible 1- and 2-cycles. Middle line: taking the vertices in increasing label, one can draw incrementally the cylindric triangulation. Bottom line: dealing with chordal edges.

contains v. Then (again by minimality of Γ' and maximality of Γ''), Γ_v has no cycle enclosing Γ''. Hence (in the annular representation of G'), there is a closed curve γ that meets G' only at the vertices v', v'' and whose interior is made of the edges of Γ_v only (so γ does not enclose Γ''). Such a curve yields a 2-separator in the periodic representation of G, a contradiction.

5   Allowing for non-contractible 1- and 2-cycles

A cylindric map with non-boundary faces that are triangles is called a *weakly simple* cylindric triangulation if cycles of length 1 or 2 have to separate the two boundary-faces, and if each vertex is incident to at most one loop. A toroidal map with triangular faces is called a *weakly simple* toroidal triangulation if cycles of length 1 or 2 are non-contractible and if there are no parallel loops incident to the same vertex. These are the necessary and sufficient conditions for the map to have no loop nor multiple edges in the periodic representation (hence these are the conditions under which one can aim at a periodic crossing-free straight-line drawing). For weakly simple cylindric triangulations without loops (nor chords incident to B_1), exactly the same shelling procedure and iterative drawing algorithm can be taken as for simple cylindric triangulations. In case there are loops we have to explain how to deal with them. For the shelling procedure, if the current upper boundary C_k is a loop —call v the incident vertex— then one deletes the loop and immediately takes v as the next free vertex (the fact that v is free is due to the fact that there is no other loop at v). In the drawing procedure (how to insert v and its incident loop into the drawing), one first adds v without its loop (by a classical one-step iteration of the drawing algorithm, involving two strip insertions), and then one draws the loop at v as an horizontal segment spreading over the whole width of the current periodic drawing (no strip insertion is done to draw the loop). Finally one can deal with chords incident to B_1 in the same way as for simple cylindric triangulations. About weakly simple toroidal triangulated maps, the procedure

is also the same as for simple toroidal triangulations, since the above proof of existence of a tambourine holds in that case. And the grid bounds (whether for the cylindre or for the torus) are the same as for simple triangulations.

Acknowledgments

References

[1] M. O. Albertson and J. P. Hutchinson. On the independence ratio of a graph. *J. Graph. Theory*, 2:1–8, 1978.

[2] N. Bonichon, C. Gavoille and A. Labourel. Edge partition of toroidal graphs into forests in linear time. In *ICGT*, volume 22, pages 421–425, 2005.

[3] E. Brehm. 3-orientations and Schnyder 3-Tree decompositions. Master's thesis, FUB, 2000.

[4] E. Chambers, D. Eppstein, M. Goodrich, M. Loffler. Drawing graphs in the plane with a prescribed outer face and polynomial area. In *GD*, pages 129–140, 2011.

[5] L. Castelli-Aleardi, E. Fusy, and T. Lewiner. Schnyder woods for higher genus triangulated surfaces, with applications to encoding. *Discr. & Comp. Geom.*, 42(3):489–516, 2009.

[6] C. Duncan, M. Goodrich, S. Kobourov. Planar drawings of higher-genus graphs. *Journal of Graph Algorithms and Applications*, 15:13–32, 2011.

[7] H. de Fraysseix, J. Pach and R. Pollack. How to draw a planar graph on a grid. *Combinatorica*, 10(1):41–51, 1990.

[8] D. Gonçalves and B. Lévêque. Toroidal maps : Schnyder woods, orthogonal surfaces and straight-line representation. arXiv:1202.0911, 2012.

[9] S. J. Gortler, C. Gotsman and D. Thurston Discrete one-forms on meshes and applications to 3D mesh parameterization. *Computer Aided Geometric Design*, 23 (2): 83–112, 2006.

[10] G. Kant. Drawing planar graphs using the canonical ordering. *Algorithmica*, 16(1):4–32, 1996.

[11] W. Kocay, D. Neilson and R. Szypowski. Drawing graphs on the torus. *Ars Combinatoria*, 59:259–277, 2001.

[12] B. Mohar. Straight-line representations of maps on the torus and other flat surfaces. *Discrete Mathematics*, 15:173–181, 1996.

[13] B. Mohar and P. Rosenstiehl. Tessellation and visibility representations of maps on the torus. *Discrete & Comput. Geom.*, 19:249–263, 1998.

[14] W. Schnyder. Embedding planar graphs on the grid. In *SoDA*, pages 138–148, 1990.

[15] A. Zitnik. Drawing graphs on surfaces. In *SIAM J. Disc. Math*, 7(4):593–597, 1994.